Supplementary material for LHCb-PAPER-2015-041

A Differential cross-sections

Figures 1 and 2 show the D^0, D^+, D_s^+, and D^{*+} cross-section measurements comparing the $p_{\rm T}$ dependence of the different rapidity ranges.

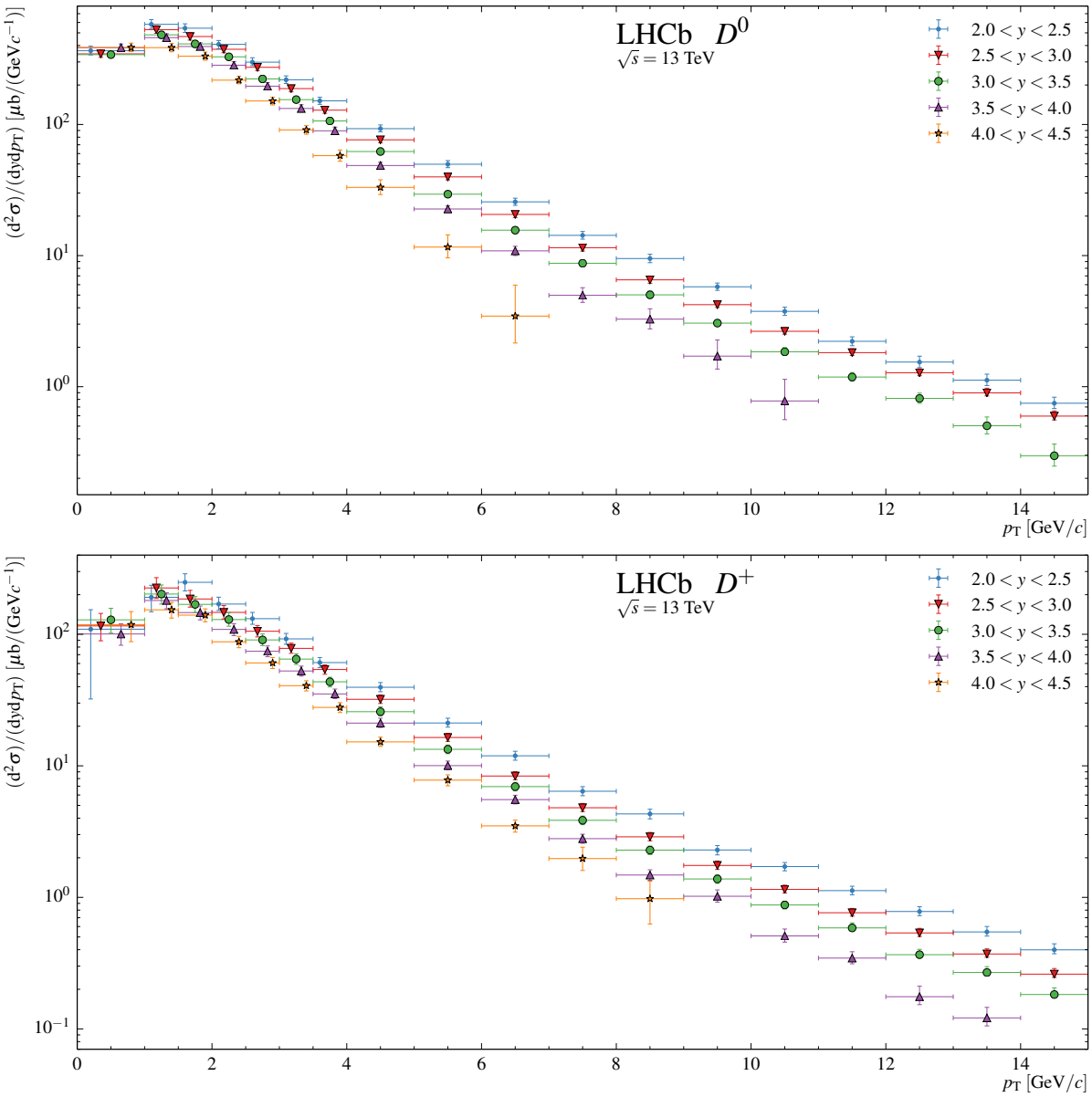

Figure 1: The differential prompt (top) D^0, and (bottom) D^+ cross-sections at $\sqrt{s} = 13\,\text{TeV}$ as described in Sec 4. The plotted p_T values below $p_\text{T} = 4$ GeV/c have been displaced within each bin for better visibility.

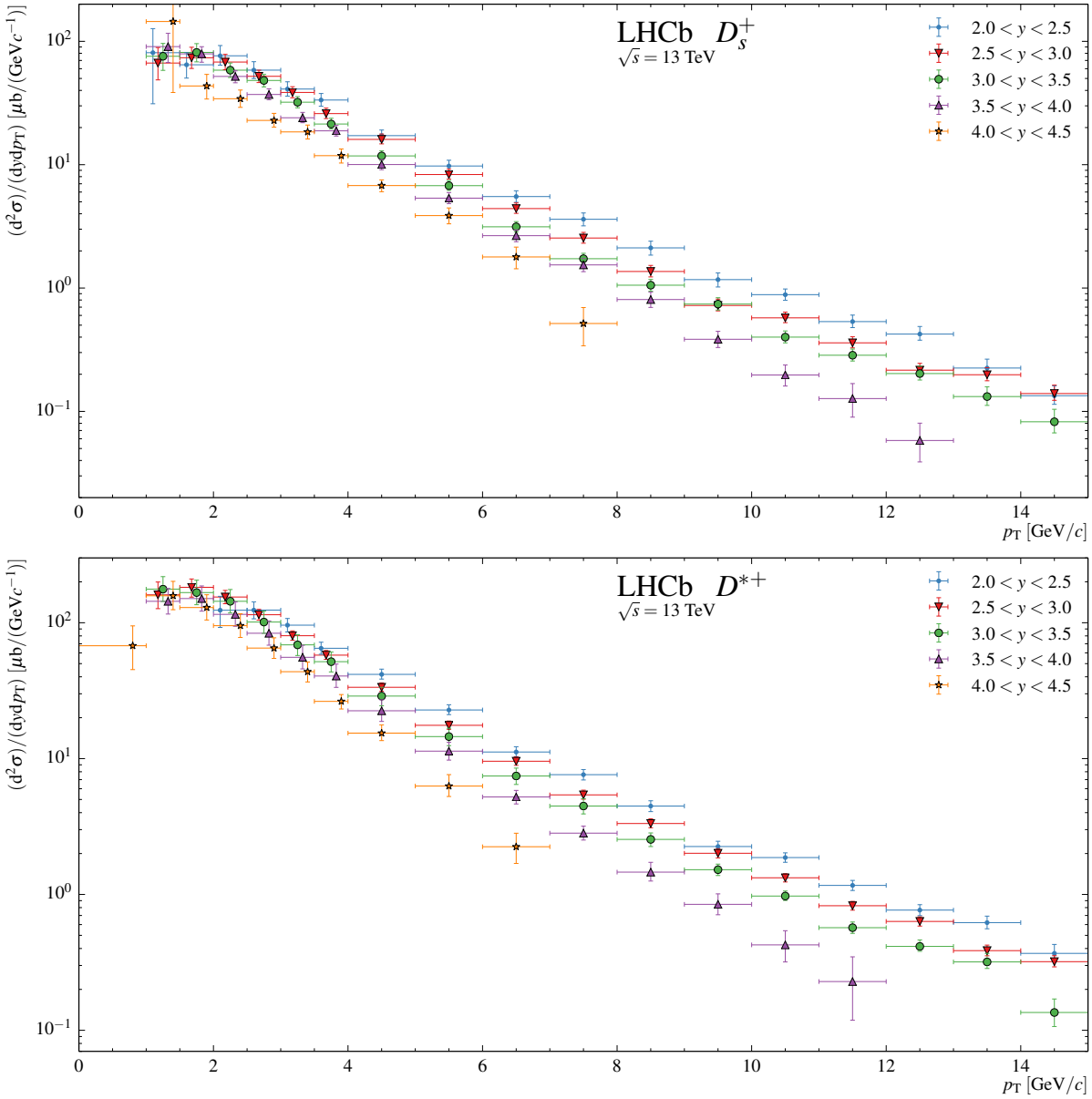

Figure 2: The differential prompt (top) D_s^+, and (bottom) D^{*+} cross-sections at $\sqrt{s} = 13\,\text{TeV}$ as described in Sec 4. The plotted p_T values below $p_T = 4$ GeV/c have been displaced within each bin for better visibility.

B Single-differential cross-section ratios

Figures 3 and 4 show the D^0, and D^+ cross-section ratios of $\sqrt{s} = 13$ to 7 TeV data as a function of $p_{\rm T}$ and y, respectively. The cross-sections are integrated over the range $2.0 < y < 4.5$ in Fig. 3 and over $0 < p_{\rm T} < 8$ GeV/c in Fig. 4. Empty bins indicate that there are missing measurements within the integration range and no extrapolation is employed to circumvent this. Hence the entries in Fig. 3 cover the full range in y while there are insufficient measurements to provide data points for all bins in y in Fig. 4. This explains the difference in the average values between the two figures.

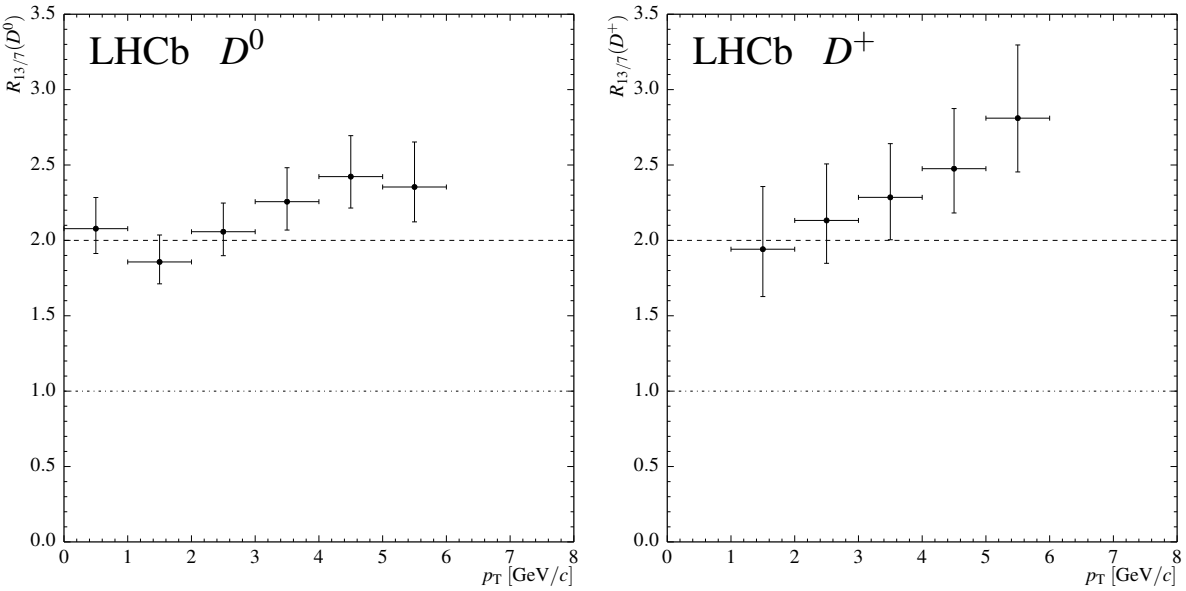

Figure 3: Cross-section ratios of $\sqrt{s} = 13$ to 7 TeV data as a function of $p_{\rm T}$ for (left) D^0, and (right) D^+.

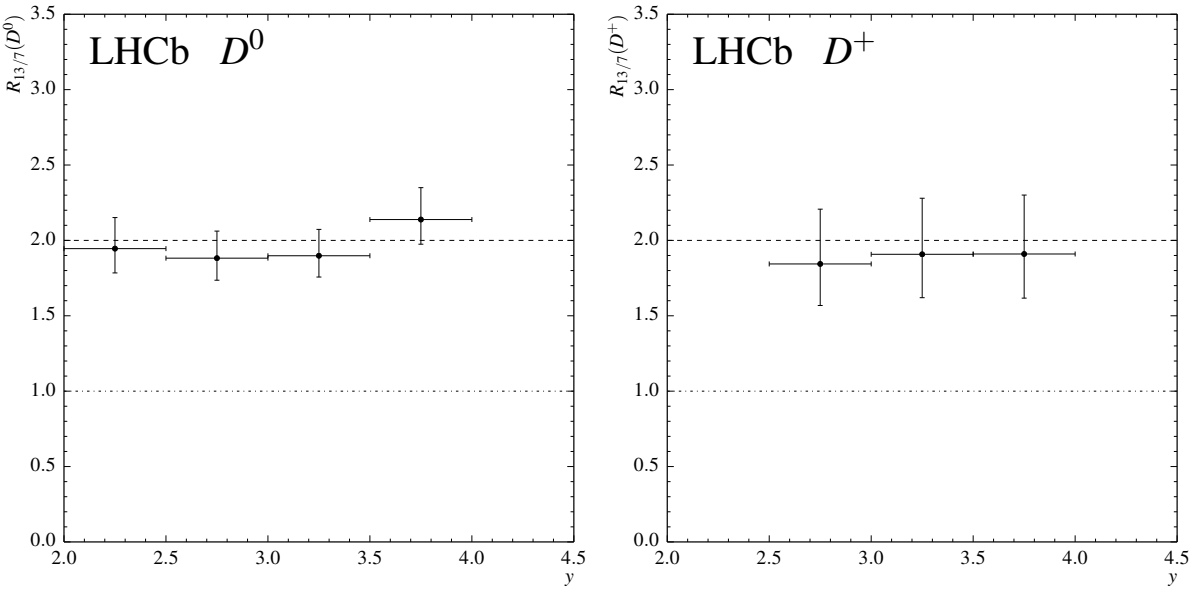

Figure 4: Cross-section ratios of $\sqrt{s} = 13$ to 7 TeV data as a function of y for (left) D^0, and (right) D^+.